BOUNDARY CONDITIONS FOR THE INDUSTRIAL PRODUCTION OF LFC CELLS
RESULTS FROM THE JOINT PROJECT INKA

A. Grohe[1], J. Catoir[1], B. Fleischhauer[1], R. Preu[1], S. W. Glunz[1], G. P. Willeke[1]
E. Schneiderlöchner[2], R. Lüdemann[2], J. Liu[3], S. Schramm[3], R. Trassl[3], S. Wieder[3],
[1] Fraunhofer Institute for Solar Energy Systems (ISE), Heidenhofstrasse 2, D-79110 Freiburg, Germany
[2] Deutsche Cell GmbH, Berthelsdorfer Strasse 111A, D-09599 Freiberg / Sachsen, Germany
[3] Applied Materials GmbH & Co. KG, Siemensstrasse 100, 63755 Alzenau, Germany

ABSTRACT: In this paper we report about some results achieved in the joint project named INKA ("**In**-line **K**ontaktierung mittels physikalischer Gasphasen-**A**bscheidung" i.e. "inline contacting by gas phase deposition") conducted by Fraunhofer ISE, Deutsche Cell and Applied Material (formerly Applied Films). We evaluated the feasibility of sputtering processes for the solar cell production as well as its application for the Laser-Fired Contacts (LFC) approach. In detail we present evaluations for the rear metallisation technology feasible to deposit sufficiently thick aluminum layers. Furthermore some high efficiency solar cell results achieved during this metallisation process evaluation are presented. Finally this knowledge was applied to produce industrial-type solar cells featuring a sputtered silicon nitride rear side passivation layer as well as 2 μm of aluminum contacted by LFC with a maximum efficiency of 16.7 %.
Keywords: manufacturing and processing, laser processing, back contact

1 INTRODUCTION

Most advanced solar cell concepts like the passivated emitter and rear cell (PERC), especially with its realizations of the back contacts by Laser-Fired Contacts (LFC) [1] feature a passivation layer covering most of the rear side of the solar cell surface. Screen-printed rear side metallisation techniques are generally not tolerated by these passivation layers due to their need for a high temperature firing step for contact formation. Therefore a rear side metallisation technology like evaporation or sputtering has to be chosen. This technology has to be capable to deposit at least 2-3 μm [2] of aluminum at reasonable cost and must not significantly harm the rear side passivation layer quality.

We performed numerous experiments regarding the deposition process itself. On one hand we compared different evaporation and sputtering processes with respect to their influence on the solar cell parameters. On the other hand we evaluated the influence of the aluminum purity on any possible contamination of the solar cells. Finally some industrially processed LFC solar cell results are presented.

2 ALUMINUM PURITY

2.1 Motivation

For most evaporation or sputtering targets prices vary drastically depending on the purity of the metal used. Usually the nomenclature for the quality of the material is given by the number of nines being used when describing the purity of the metal, e.g. 2N for 99 % or 4N6 for 99,996 %. Aluminum is commercially available in a range up to 5N, with standard values for foils or sheets around 3N to 4N. For this experiment we used two different purity levels, 3N8 Al as a cheap alternative to the 5N Al being used as reference. The major contaminations in the used 3N8 Al are silicon with a concentration of 30 ppm as well as copper and iron with a concentration of 20 ppm. For 5N Al all metal contaminations range below 1 ppm. Even though the difference in purity seems to be only little its impact on

the material price is more than one magnitude, leading to a cost reduction from ~300 Euro/kg for 5N Al to ~10 Euro/kg for 3N8 respectively [3].

2.2 Solar cell test structure

To evaluate the impact of the impurities contained in the evaporation target we used our standard high efficiency solar cell structure. This structure leads to efficiencies around 21 % with a very narrow distribution within one run due to the high process reproducibility. It features seven 20×20 mm² solar cells distributed evenly on a 4 inch Float Zone wafer with a base resistivity of 1 Ω cm. The cells feature a random pyramid front side texture and a 120 Ω/sq. POCl₃ diffused emitter. The front side passivation as well as the antireflection coating is established by 105 nm of thermally grown silicon dioxide. The front contacts consist of an evaporated contact composed of titanium, palladium and silver. These contacts are placed into photolithographically defined openings by lift-off technology and thickened by electroplating. On the rear side we deposit 2 μm of evaporated aluminum on top of the 105 nm thermally grown silicon oxide. The aluminum is alloyed into the silicon base of the solar cell using Laser-Fired Contacts (LFC). Finally all samples were annealed at 425 °C for 25 minutes [2].

We processed five wafers in total. They are split into three references evaporated with 5N aluminum as well as two samples evaporated with impure 3N8 aluminum. After the measurement of the samples the arithmetic mean was taken to compare the influence of the aluminum purity amongst each other.

2.3 Solar cell results and discussion

The results of the processed solar cells are shown in table 1. The values for 3N8 Al represent the solar cells processed on two wafers (14 cells) whereas three wafers (21 cells) were processed with 5N Al. All values are measured after the final annealing step.

For both materials used an average efficiency of 20 % was obtained. No significant difference can be observed. Therefore the aluminum purity of the evaporated metallisation layer does not seem to have a

major influence within the impurity range evaluated. As even the final annealing step does not show any impact on the solar cell performances it can be posted that the impurity concentrations being present in the 3N8 Al were not high enough to decrease the values sufficiently.

Table 1: Solar cell results of the evaporation metal purity experiment. The values for 3N8 Al are calculated from 14 cells whereas the 5N Al values represent 21 samples.

purity [%]	V_{OC} [mV]	J_{SC} [mA/cm²]	FF [%]	η [%]
99,98	661.3±2.6	39.0±0.1	77.8±0.4	20.1±0.2
99,999	660.1±2.3	39.1±0.2	77.5±2.0	20.0±0.5

3 METALLISATION TECHNIQUE COMPARISON

3.1 Purpose of the study

In order to determine the ideal metallisation technique for an industrial application of a deposited metal layer we compared different approaches for the physical vapor deposition (PVD) of the aluminum. On one hand standard evaporation techniques were studied splitting into thermal evaporation and e-gun evaporation. In the first case the whole aluminum reservoir gets heated high enough to evaporate while in the latter case an electron beam is used to heat and evaporate the aluminum locally. Evaporation usually is regarded to be gentle but also to generate thermal impact on the samples. On the other hand we used sputtering. Here aluminum parts are removed from a target by high energy ions and then deposited on the substrate. Sputtering generally is regarded to exhibit a superb homogeneity but also to induce surface damage.

Both approaches are feasible for the deposition of the aspired layer thickness of approximately 2 µm.

3.2 Design of experiment

Once again we used our high efficiency solar cell structure for this evaluation. Like in the previous experiment seven 20x20 mm² solar cells are placed on a 4 inch Float Zone wafer with a base resistivity of 1 Ω cm. The whole setup of the cells including texturisation, emitter diffusion, front side metallisation and passivation was identically with the previous experiment as well.

For the rear side metallisation we used two wafers at a time for the three different PVD techniques. All samples were measured prior to the final annealing step at 425 °C for 25 minutes as well as afterwards to evaluate the influence of the final temperature treatment on the potential damage induced by the metallisation.

3.3 Solar cell results and discussion

The solar cell results of the PVD technology comparison are shown in table 2. All values displayed represent the arithmetic means as well as the standard deviations of 14 solar cells (placed on two different wafers) prior and past the final annealing step. Furthermore the graphs for the reflection, external and internal quantum efficiency are shown in figure 1. Here we chose to measure and compare only the best sample of each PVD method.

Table 2: Solar cell results of the PVD technology comparison. All values are shown prior (1) and after (2) the final annealing step and represent the arithmetic mean of 14 samples.

rear side	V_{OC} [mV]	J_{SC} [mA/cm²]	FF [%]	η [%]
E-Gun 1	615.1±3.4	35.7±0.2	78.2±2.4	17.2±0.6
E-Gun 2	675.4±5.5	39.4±0.3	78.5±2.3	20.9±0.8
Thermal 1	644.7±6.5	37.9±0.3	78.7±0.2	19.2±0.3
Thermal 2	677.3±3.5	39.4±0.3	78.4±1.0	20.9±0.5
Sputter 1	637.5±1.2	37.6±03	78.4±0.6	18.8±0.2
Sputter 2	669.4±1.7	39.0±0.4	78.8±0.5	20.6±0.3

All fill factors of all samples are on the same level. This supports that there is not any identical influence of the aluminum layers deposited differently on the LFC process itself. When comparing the values of the open circuit voltage as a measure of the damage induced by the metallisation process thermal evaporation performs best followed by sputtering (- 7 mV) and e-gun evaporation (-30 mV). We assume that the radiation emitted by the e-gun source and the sputtering target are responsible for the loss in V_{OC}, respectively.
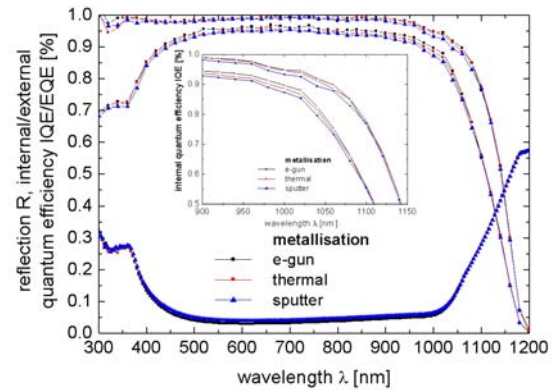
Figure 1: Reflection, internal and external quantum efficiency of three solar cells with aluminum being deposited by different PVD techniques. The inlay shows the region of the IQE representative for the rear side.

When performing the annealing process to enhance the passivation layer quality as well as the laser induced damage all values rise drastically. For thermally evaporated aluminum the deviation is ~33 mV denoting the absolute level of the healing effects mentioned above. This lift is observable for both other metallisation methods as well with an additional gain of ~30 mV for the case of e-gun evaporation. The samples for this PVD method end on an equivalent level. For the sputtering technique no additional gain to the ~30 mV is observable keeping the loss at ~7 mV relative to the evaporation methods. The results imply that the damage caused by the e-gun evaporation can be annealed by the specific annealing step while this is not the case for sputtering.

3.4 Further analysis of the sputtering method

As magnetron sputtering was used for the experiments in 3.3 no efficiency loss of the solar cells due to any sputtering influence was expected. Therefore we performed the identical experiment with a slightly different sputtering

equipment placed at Applied Materials in Alzenau, Germany. Once again we used the identical high efficiency solar cell test structure like in the previous experiments. This time we processed three wafers with a total of 21 solar cells with sputtered aluminum and just one wafer with seven solar cells as reference with thermal evaporation. The results of this experiment are shown in table 3.

Once again we measured the solar cell parameters before (denoted by "1") and after (denoted by "2") the final annealing step to evaluate the influence on any potential damage. As can be seen in table 3 the adaptation of the sputtering process lead to an value of V_{OC} equaling the one achieved by thermal evaporation. A negligible variation in the electroplating process could be responsible for the deviations of J_{SC} and fill factor in the opposite direction. Nevertheless the final solar cell efficiency of both PVD technologies is equal.

Table 3: Solar cell results for the second sputtering metallisation experiment before (1) and after (2) sintering. The reference values represent seven cells whereas the sputtering ones cover 21 cells.

rear side	V_{OC} [mV]	J_{SC} [mA/cm²]	FF [%]	η [%]
Ref 1	614.0±0.9	36.4±0.1	78.1±0.2	17.5±0.1
Ref 2	669.4±3.8	39.8±0.1	77.0±0.7	20.5±0.3
Sputter 1	619.5±1.4	36.7±0.2	78.1±0.5	17.8±0.2
Sputter 2	670.1±3.5	39.0±0.3	78.7±1.0	20.6±0.5

Due to the process stability within one batch the solar cell parameters can be compared very good within the same batch. Unfortunately even slight process variations lead to different results on this high level. Therefore the comparison between different batches (e.g. the results in table 2 or 4) is not recommendable.

4   PATH TO INDUSTRIAL REALIZATION

4.1 Motivation and boundary conditions

We have already shown in section 3 that several different metallisation techniques like sputtering and evaporation are feasible in principle. For the industrial application one further important aspect has to be taken into account: the deposition rate. Standard LFC contacts require an aluminum layer thickness of approximately 2-3 µm [4].

Two ways can be chosen to achieve this goal, on one side the enlargement of the deposition rate and on the other side the extension of the deposition equipment with further deposition chambers. For the experiment we used a high-deposition rate system at Applied Materials in Alzenau, Germany. This machine usually coats plastic films at a speed of ??? with a thin aluminum layer being used in food wrapping for example. The equipment setup was slightly changed in order to match the demands of wafer coating. With adjustments to the machine setup lower and higher values of the deposition rate are easy to realize as well.

4.2 Solar cell results

To evaluate the quality of the aluminum deposited with high evaporation rates we once again used our high efficiency solar cell test structure described in 2.2. This time we deposited a total of four wafers with approximately 2 µm of aluminum using the high evaporation rate process divided into two runs. One sample was evaporated with the ISE standard process and used as reference. The values of these cells are shown in table 4.

Table 4: Solar cell parameters after annealing for the experiment with high and low deposition rates. The values of the solar cells evaporated with a high rate represent the arithmetic mean of 28 cells, the low rate represents only 7 cells.

rate	V_{OC} [mV]	J_{SC} [mA/cm²]	FF [%]	η [%]
high	680.2±3.8	39.8±0.3	78.2±2.5	21.2±0.8
low	680.9±2.8	39.9±0.3	78.2±1.2	21.3±0.6

The values match each other very well. Within the measurement tolerance there is no difference visible leading to the conclusion that aluminum evaporation with higher deposition rates is feasible for solar cell processing as well.

5   INDUSTRIAL LFC CELL PRODUCTION SCHEME

5.1 Process sequence

One further aim of the joint project was to demonstrate the feasibility of at least one possible route for the industrial production of LFC solar cells. Therefore we used wafers being partly industrially processed by Deutsche Cell, Freiberg, Germany. The base material was p-type monocrystalline Czochralksi silicon in the size of 125x125 mm². The wafers were industrially textured and emitter diffused. Finally the front side was covered by a silicon nitride antireflection coating.

Those partly processed wafers were then further completed at Fraunhofer ISE. As a first step the parasitic emitter was removed from the rear sides. Immediately after conditioning the rear sides all samples were coated on the rear side by various sputtered silicon nitride layers acting as passivation. The front side of the samples then were screen-printed using a standard grid design and fired in an inline fast firing furnace. For the rear metallisation we used the aluminum evaporation process at Applied Materials, Alzenau, Germany which was evaluated in section 4 as well as our slower reference process at Fraunhofer ISE. Finally the samples were laser processed at Fraunhofer ISE to establish the LFC contacts. The final sintering step was performed in an inline belt furnace enabling the same effect as the quartz tube forming gas process [2].

5.2 Solar cell results

In table 5 an overview over some of the results achieved with the process mentioned above is given.

Two passivation layers showed promising performance. The denotation here 'VL' and 'L' stands for the hydrogen content of the sputtered silicon nitride rear side passivation layer whereas all other process parameters were kept identical. Together with the contact

firing temperature which is denoted by 'T$_1$' to 'T$_5$' they mark the rear side passivation type. This temperature was varied over a range of 60 °C, whereas 'T$_1$' represents the lowest value and 'T$_5$' the highest one. Values marked by * are measured on a 100×100 mm² area. All values named with 'ave.' represent arithmetic mean values of the sample amount mentioned in brackets. The mean value of all 15 VL passivated samples is given as well.

Table 5: Measured parameters of some exemplary solar cells. 'VL' and 'L' denote the hydrogen content of the rear side passivation, together with the contact firing temperature 'T$_1$' to 'T$_5$' they mark the rear side passivation type. All values named with 'ave.' represent arithmetic mean values of the sample amount mentioned in brackets. Values marked by * are measured on a 100×100 mm² area.

sample	type	V$_{OC}$ [mV]	J$_{SC}$ [mA/cm²]	FF [%]	η [%]
VL best	VL-T$_1$	621.8	35.9	72.9	16.3
L best	L-T$_2$	619.3	35.8	72.7	16.1
L best*	L-T$_2$	617.3*	35.6*	76.0*	16.7*
ave. (3)	VL-T$_1$	621.4	35.8	72.0	16.0
ave. (3)	VL-T$_2$	619.1	35.8	71.9	15.9
ave. (3)	VL-T$_3$	618.5	35.8	71.7	15.9
ave. (3)	VL-T$_4$	618.5	35.8	71.7	15.9
ave. (3)	VL-T$_5$	617.0	35.4	72.6	15.9
ave. (15)	VL-T$_{all}$	618.9 ± 2.0	35.7 ± 0.2	72.0 ± 0.7	15.9 ± 0.2

Obviously all samples lack in fill factor, with the open circuit current being improvable as well. The independence of the solar cell parameters from the contact firing temperature probably results from this lack of fill factor. Still it shows a very good process stability, unfortunately on an unsatisfying level. This behavior was observed earlier already, the reason is currently under investigation.

The silicon nitride rear side passivation layer used for this experiment lead to good effective surface recombination velocities S$_{eff}$ of approximately 100 cm/s. However, we believe that due to the composition of the silicon nitride layer there should not occur significant problems with inversion channels [5].

Some improvement in fill factor can be achieved by cutting the samples to a reduced size. The rise of > 3% absolute in fill factor lifts the solar cell efficiency to a more satisfying level. Nevertheless we chose not to enhance our measurements by performing this process on more prospective samples as well as we still perform deeper analysis and characterization. Still the results show a very promising path for the industrial realization of large sized LFC solar cells, processed only with the use of industrial proven or in principle feasible processes and with silicon nitride acting as rear side passivation layer.

6 SUMMARY AND CONCLUSION

After numerous experiments concerning the metallisation method and its adaption to the special needs of crystalline silicon solar cells we found that:
- within the range of 99,98 to 99,999 % of aluminum purity we did not find an significant influence of the contamination contained in the evaporation targets measurable. This decreases the material costs by more than one order of magnitude.
- All three metallisation methods examined are feasible for the deposition of aluminum on the rear side of a LFC solar cell. This includes thermal evaporation, e-gun evaporation as well as sputtering. Thermal evaporation exhibits the lowest influence, e-gun evaporation the highest one. With good process optimization and the necessary post-annealing step all methods lead to the same maximum efficiency level.
- For industrial production the throughput of a metallisation system and therefore its deposition rate is crucial. To demonstrate one possibility of a process close to these industrial demands we evaluated an evaporation method leading to very high deposition rates without having any effect on the solar cell performance at all.
- Finally some large area solar cells were processed using solely industrially feasible and established processes leading to efficiencies of 16.7 %.

REFERENCES

[1] R. Preu, E. Schneiderlöchner, S. Glunz et al., world patent application, 2001
[2] A. Grohe, B. Fleischhauer, R. Preu, S.W. Glunz, G.P. Willeke, WCPEC 4, Waikoloa, Hawaii, USA (2006) in print
[3] Umicore, material specifications, Umicore Materials, 2005
[4] A. Grohe, E. Schneiderlöchner, B. Fleisch-hauer, M. Hofmann, S.W. Glunz, R. Preu and G. Willeke, EUPVSEC 21, Barcelona, Spain (2005) in print.
[5] S. Dauwe, L. Mittelstädt, A. Metz, R. Hezel, 17th EC PVSEC, Munich, Germany, pp. 339-342